REPORT DOCUMENTATION PAGE

Form Approved
OMB No. 0704-0188

The public reporting burden for this collection of information is estimated to average 1 hour per response, including the time for reviewing instructions, searching existing data sources, gathering and maintaining the data needed, and completing and reviewing the collection of information. Send comments regarding this burden estimate or any other aspect of this collection of information, including suggestions for reducing the burden, to Department of Defense, Washington Headquarters Services, Directorate for Information Operations and Reports (0704-0188), 1215 Jefferson Davis Highway, Suite 1204, Arlington, VA 22202-4302. Respondents should be aware that notwithstanding any other provision of law, no person shall be subject to any penalty for failing to comply with a collection of information if it does not display a currently valid OMB control number.

PLEASE DO NOT RETURN YOUR FORM TO THE ABOVE ADDRESS.

1. REPORT DATE *(DD-MM-YYYY)*	2. REPORT TYPE	3. DATES COVERED *(From - To)*
26-02-2008	Final Performance Report	From 26-02-2008 To 16-02-2012

4. TITLE AND SUBTITLE
QUANTUM SIMULATION OF THE HUBBARD MODEL USING ULTRA-COLD ATOMS

5a. CONTRACT NUMBER

5b. GRANT NUMBER
FA9550-08-1-0069

5c. PROGRAM ELEMENT NUMBER

6. AUTHOR(S)
Dr. Kenneth M O'Hara

5d. PROJECT NUMBER

5e. TASK NUMBER

5f. WORK UNIT NUMBER

7. PERFORMING ORGANIZATION NAME(S) AND ADDRESS(ES)
Pennsylvania State University | Eberly College of Science | Department of Physics
104 Davey Lab, #195 | Office 152H
University Park, PA 16802-6300 (USA)

8. PERFORMING ORGANIZATION REPORT NUMBER

9. SPONSORING/MONITORING AGENCY NAME(S) AND ADDRESS(ES)
AFOSR / RSE
875 North Randolph Street, Suite 325
Room 3112
Arlington, Virginia 22203-1768

10. SPONSOR/MONITOR'S ACRONYM(S)
AFOSR / RSE

11. SPONSOR/MONITOR'S REPORT NUMBER(S)
AFRL-OSR-VA-TR-2012-0633

12. DISTRIBUTION/AVAILABILITY STATEMENT
1) DISTRIBUTION STATEMENT A: Approved for public release; distribution is unlimited

13. SUPPLEMENTARY NOTES

14. ABSTRACT
Here we report on the successful creation of a quantum degenerate, three-component Fermi gas of atoms. We also report on our observation of resonances in the three-body recombination rate in this gas which indicate the formation of Efimov trimer states. The three-component Fermi gas we have created will, when confined in an optical lattice, be an experimental realization of the SU(3) Hubbard model. The SU(3) Hubbard model has been proposed as a model system for studying different phases of matter expected to occur in quantum chromodynamics (QCD): the color superconducting phase and the formation of baryons. Our initial investigations have focused on understanding three-body recombination in this system. Three-body recombination is of interest as it will be the limiting factor in determining our lowest temperatures. Three-body recombination can also be used to test universal predictions for the quantum three-body problem such as the Efimov effect. We have already observed two resonant features which indicate the formation of Efimov trimer states and are currently testing predictions of Efimov¿s theory when the scattering length is

15. SUBJECT TERMS
QUANTUM SIMULATION; HUBBARD MODEL; ULTRA-COLD ATOMS

16. SECURITY CLASSIFICATION OF:			17. LIMITATION OF ABSTRACT	18. NUMBER OF PAGES	19a. NAME OF RESPONSIBLE PERSON
a. REPORT	b. ABSTRACT	c. THIS PAGE			Tatjana Curcic, RSE (Program Manager)
U	U	U	UU		19b. TELEPHONE NUMBER *(Include area code)* 703.696.6204

Crawley, Erin CTR USAF AFMC AFOSR/NE

From: Ken O'Hara [kohara@phys.psu.edu]
Sent: Thursday, November 06, 2008 12:35 PM
To: Curcic, Tatjana Civ USAF AFMC AFOSR/NE; Crawley, Erin CTR USAF AFMC AFOSR/NE
Cc: gag14@psu.edu
Subject: Annual Report Due Date
Attachments: 123082_2.tif; ThreeStateMixture.pdf; FilterCooling.pdf; PhysicsTodaySaDeMelo.pdf

Dear Tatjana and Erin,

I'm writing because I am a bit confused about when my annual report for Award No. FA9550-08-1-0069 is due. A document I was sent when I received the award seems to indicate that nothing is due until Feb. 2009 (see the end of attached document 123082_2.tif). However, my recollection from previous years is that annual reports for AFOSR have been due in the Fall. Please let me know if you need something before Feb. 28 2009. We have been getting great results in the lab and it would be easy to put something together immediately if you need it.

I also wanted to take this opportunity to ask whether everything looks good for funding Option 1 of this award. Please let me know if there are any anticipated problems or delays.

I also wanted to give a brief update on the results we've been getting in the laboratory... We have been experimentally investigating three-state mixtures of degenerate Fermi gases. Using these mixtures we can confirm theoretical predictions for the quantum 3-body problem. In the longer term (~1 to 2
yrs.) we will confine this mixture in an optical lattice and simulate the SU(3) Hubbard model and high density quark matter described by quantum chromodynamics.

We have been investigating the stability of the 3-state Fermi gas with respect to decay due to three-body recombination. The three-body recombination rate is an observable we can use to compare to theoretical predications based on solutions to the quantum 3-body problem. Understanding the stability of the gas also has important implications for the feasibility of future studies of quantum chromodynamics in this system. We have been working with Eric Braaten, a high energy physics theorist at Ohio State University, to interpret our data. Eric has been able to fit our results using a three-body model with only 2 free parameters. His results indicate that our results are in agreement with predictions made by Vitaly Efimov, a Russian nuclear physicist, over 35 years ago. Futhermore, Eric's results predict that we should be able to perform even more stringent tests of Efimov's predictions in experiments we are performing right now. These results will be of interest in several subfields of physics including nuclear, high-energy, atomic, molecular and particle physics as well as quantum chemistry.

Our results also indicate that the observation of BCS superfluidity in this system should be possible. The superfluid phase in this system would be analogous to the color superconducting phase predicted to occur inside neutron stars. The possiblity for such future studies was highlighted in the October issue of Physics Today (see attached article). We have submitted our recent results to PRL (see attachment).

We also recently submitted our proposal for cooling fermions in an optical lattice to PRL (see attachment).

Our experimental capabilities have improved. In addition to being able to produce degenerate Fermi gases composed of 2 or 3 spin states, we can also produce molecular Bose-Einstein condensates in our laboratory which are composed of Li dimer molecules. This allows us to get to extremely low temperatures.

We have also developed and demonstrated a novel ring laser source. In collaboration with Stephen Gensemer, a former postdoc in Kurt Gibble's lab, we have demonstrated a new method for obtaining uni-directional single-frequency operation of a high-power ring laser by a technique we call self injection locking. This technique can be applied to any ring laser and therefore will be of broad interest to any research/industrial application which uses high-power single frequency ring lasers. We are in the process of writing these results up and plan to submit a paper to Nature Photonics.

Please let me know if you need an official performance report prior to Feb 28, 2009. As I said, I can get something to you quickly if necessary. If the report is already delinquent, I'm sorry for the confusion and I will get it in immediately.

Best regards,
Ken

--
Kenneth M. O'Hara
Assistant Professor of Physics
Penn State University
104 Davey Lab, PMB 195
University Park PA 16802
Phone: 814-865-7259
FAX: 814-865-3604
e-mail: kohara@phys.psu.edu

feature article

When fermions become bosons: Pairing in ultracold gases

Carlos A. R. Sá de Melo

The unprecedented control over the interactions and pairing of ultracold fermionic atoms provides insight into exotic strongly correlated phenomena and illuminates the physics of superfluidity in metals, nuclei, and neutron stars.

Carlos Sá de Melo is a professor of physics at the Georgia Institute of Technology in Atlanta.

If you ask an undergraduate student, "What do neutron stars, metals, nuclei, and atoms have in common?" you might hear the answer, "They are made of neutrons, protons, quarks, and electrons." While it is common for students to have heard about the existence of those microscopic particles and their individual properties like charge, spin, and color, it is far less common to hear from them that neutrons, protons, quarks, electrons, and atoms may exhibit a collective and macroscopic property called superfluidity, in which a large number of particles can flow coherently without any friction or dissipation of heat.

Neutron stars, metals, nuclei, and ultracold atoms have revealed their amazing superfluid state in ingenious experiments (see figure 1 for estimated critical temperatures of fermion superfluids). The first discovery of superfluid behavior was made nearly 100 years ago, when Heike Kamerlingh Onnes in 1911 cooled a metallic sample of mercury to temperatures below 4.2 K, using liquid helium-4 as the refrigerant, and found to his astonishment that the sample conducted electricity without dissipation. That dramatic drop in electrical resistivity to an essentially zero-resistance state was coined superconductivity, also known as charged superfluidity.

Revealed through Kamerlingh Onnes's push to reach very low temperatures, that incredible quantum phenomenon emerged several years before the formulation of Schrödinger's equation and the basic developments of quantum theory. It took nearly 50 years after the discovery of superconductivity for the development of a microscopic theory of the phenomenon. In the intervening years, many new superconductors (charged superfluids) were discovered, but only one neutral superfluid: liquid ^{4}He.

Liquid helium-4: A boson superfluid

Although individual neutrons, protons, quarks, and electrons are all fermions with spin 1/2, individual atoms and nuclei can be either bosons with an integer total spin (0, 1, 2, . . .) or fermions with half-integer spin (1/2, 3/2, 5/2, . . .), depending on the number of their constituent fermions. The neutral atoms of ^{4}He, comprising an even number of fermions (two protons, two neutrons, and two electrons), are bosons with total spin 0. An unusual maximum in the density of liquid ^{4}He had been observed as early as 1910 (and measured again in 1922) in Kamerlingh Onnes's laboratory, and a possible discontinuity in the latent heat near the same temperature was noted in 1923 in the same laboratory, but the significance of those anomalies was not fully realized until the late 1930s. Experimental evidence for superfluid behavior in ^{4}He emerged only in 1938 when two independent measurements of viscosity were reported, one by Pyotr Kapitsa and the other by John Allen and Donald Misener; the measurements indicated exceedingly low, essentially vanishing viscosity below 2.2 K, the temperature at which the density and latent-heat anomalies of liquid ^{4}He appeared. Not long after that discovery, Fritz London[1] suggested the connection between superfluidity and Bose–Einstein condensation (BEC).

The idea of boson condensation was put forth by Albert

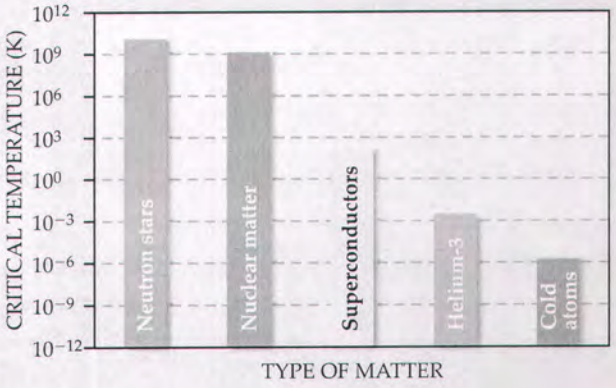

Figure 1. Fermionic superfluidity is a collective phenomenon found in neutron stars, nuclear matter, superconductors, liquid helium-3, and ultracold atoms, though they exhibit large differences in the critical temperature for the onset of superfluidity, as shown here. The key to their common behavior is the pairing of fermions to produce highly correlated fluids, which reveal themselves in several ways: They flow without dissipation, may exhibit an energy gap in the elementary excitation spectrum, have a nonclassical moment of inertia, and may exhibit vortex lattices upon rotation.

© 2008 American Institute of Physics, S-0031-9228-0810-020-5

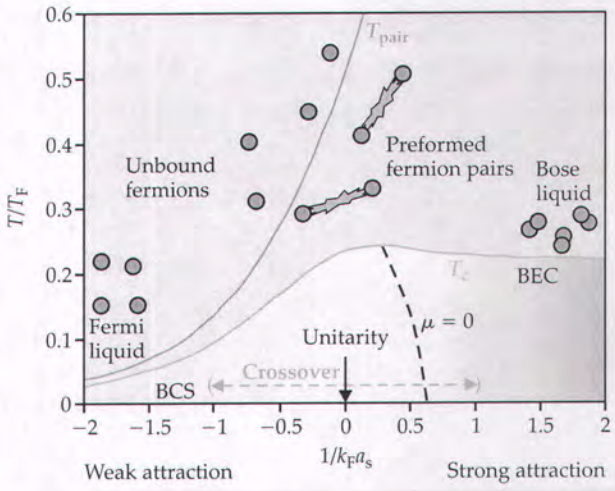

Figure 2. Phase diagram for fermionic superfluids. To see the superfluid Bardeen-Cooper-Schrieffer or Bose–Einstein condensation phases for fermions, it is necessary to cool them to a small fraction of their Fermi temperature T_F. When fermions pair to produce a superfluid state (yellow region), they exhibit two characteristic temperatures: the pairing temperature T_{pair} (pink) at which fermion pairs first form and the critical temperature T_c (blue) at which phase coherence between the pairs is established. In the BCS regime of large pairs and weak attraction, the two temperature scales are essentially the same. However, in the BEC regime of small pairs (diatomic molecules) and strong attraction, the two temperature scales are very different. The unitarity limit occurs when the scattering parameter $1/k_F a_s$ goes to zero, where k_F is the Fermi wavenumber and a_s is the scattering length, but the de facto separation between the BCS and BEC regimes is where the chemical potential μ goes to zero. (Adapted from ref. 7.)

Einstein in 1924–25, after he had read and translated a paper by Satyendra Nath Bose on the statistics of photons and had extended Bose's idea to the realm of massive bosons.[2] Einstein noted that a finite fraction (called the condensate fraction) of the total number of massive bosons would macroscopically occupy the lowest-energy (zero momentum) single-particle state at sufficiently low temperatures. For noninteracting bosons, the fraction of zero-momentum particles is 100% at zero temperature, but interactions in liquid ^{4}He are sufficiently strong to reduce the condensate fraction to 10%, even at zero temperature.

Some microscopic understanding was developed by Nikolai Bogoliubov, who demonstrated that the excitation spectrum of a weakly interacting Bose gas is linear in the momentum of the excitation and that the critical velocity—the flow speed at which superfluidity is destroyed—is finite. Bogoliubov concluded that weak repulsive interactions do not destroy the Bose–Einstein condensate, and that an ideal Bose gas in its BEC phase has a vanishing critical velocity and thus is not a superfluid. Therefore, quite generally, the formation of a Bose–Einstein condensate does not guarantee superfluidity, which is associated with the existence of currents that flow without dissipation and requires correlations—that is, interactions—between bosons.

Superconductivity and the BCS theory

Drawing from the lessons of superfluid ^{4}He and the connection to BEC, Max Schafroth proposed in 1954 that superconductivity in metals was due to the existence of a charged Bose gas of two-electron bound states—local fermion pairs—that condense below a critical temperature. However, experiments did not seem to support that simple picture. It was not until 1956 that a key idea emerged: Leon Cooper discovered that an arbitrarily small attractive interaction between two fermions (electrons) of opposite spins and opposite momenta in the presence of many others could lead to the formation of bound pairs. Since the pairing occurs in momentum space and the attraction between electrons is weak, the bound pairs, now known as Cooper pairs, are quite large and thus different from the local pairs envisioned by Schafroth. The origin of the glue between fermions was argued to be electron–phonon interactions, which could produce an effective attractive interaction between electrons that in turn could overcome their Coulomb repulsion.

The existence of a single fermion pair, however, was not sufficient to describe the macroscopic behavior of superconductors. It was still necessary to invent a collective and correlated state in which many fermion pairs acting together could produce a zero-resistance state. The invention of such a special state of matter occurred in 1957, when John Bardeen, Cooper, and Robert Schrieffer (BCS) proposed a many-particle wavefunction corresponding to largely overlapping fermion pairs with zero center-of-mass momentum, zero angular momentum (*s*-wave), and zero total spin (singlet).[3] As emphasized by BCS, their theory did not describe the picture proposed by Schafroth, Stuart Butler, and John Blatt, also in 1957, in which Bose molecules—local pairs of electrons with opposite spins—form an interacting charged Bose gas that condenses and becomes a superconductor.[4]

One of the most fundamental features of the BCS state is the existence of correlations between fermion pairs, which lead to an order parameter for the superconducting state. In the original BCS work, the order parameter was found to be directly related to the energy gap E_g in the elementary excitation spectrum. Since all relevant fermions participating in the ground state of an *s*-wave superconductor are paired, creating a single fermion excitation requires breaking a Cooper pair, but that costs energy. Thus the contribution of elementary excitations to the specific heat and other thermodynamic properties shows exponential behavior $\sim \exp(-E_g/T)$ at low temperature T. Unlike the alternative theory of Bose molecules, the BCS theory was an immediate success, since it could explain many experimental results of the time at a quantitative level.

After its great success in describing superconductors (charged superfluids), the BCS theory was quickly generalized: to higher angular momentum pairing; to neutral superfluids such as liquid ^{3}He (a fermion isotope of helium with two protons, one neutron, and two electrons), where spin-triplet *p*-wave superfluidity was found experimentally in the 1970s; and to pairing mechanisms beyond phonon mediation. But equally important were applications of the BCS theory to describe superfluid phases of fermions in nuclear matter and neutron stars, where nuclear forces provide the glue for fermion pairs. Glitches in the rotational periods of neutron stars have been attributed to the depinning of vortices—

Feshbach resonances

The evolution from a Bardeen-Cooper-Schrieffer superfluid to a Bose–Einstein condensation superfluid cannot be studied in neutron stars, nuclear matter, superconductors, or liquid helium-3, but in ultracold atoms it can be. Feshbach resonances are the tools that allow the interactions between atoms to be changed as a function of the applied magnetic field. The underlying requirement, shown schematically on the left, is that at zero magnetic field, the interatomic potentials of two atoms in their ground state (the so-called open channel) and in an excited state (the closed channel) be not too different in energy. The resonance, characterized by a divergence in the scattering length a_s, occurs when the energy difference ΔE between a bound state with energy E_{res} in the closed channel and the asymptotic, threshold energy E_{th} of scattering states in the open channel is brought to zero by an applied external magnetic field B_0. For magnetic fields B close to B_0, the background scattering length a_{bg} is renormalized to $a_s \approx a_{bg}[1 + \Delta B/(B - B_0)]$, where ΔB is the width of the Feshbach resonance. When a_{bg} is negative, a_s is positive close to the resonance for magnetic fields smaller than B_0, as seen on the right, and two fermions can form Feshbach molecules of characteristic size a_s. The most commonly studied Feshbach resonances for *s*-wave scattering occur at $B_0 = 83.4$ mT (834 gauss) for lithium-6 and at $B_0 = 22.4$ mT (224 gauss) for potassium-40, both stable fermionic isotopes.

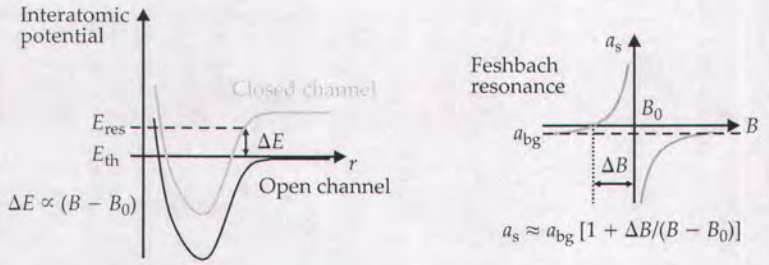

fundamental excitations of rotating superfluids—in the stars' solid crust. For some nuclei, the energy gap in the elementary excitation spectrum and the nonclassical moment of inertia indicate the existence of a superfluid state.

From BCS to BEC superfluids

Although the BCS theory and its generalizations have found applications in several areas of physics where the mechanisms for fermion pairing are quite different, it is intrinsically a weak-attraction theory. Nature was very kind to the BCS theory because it saved some of its most precious Fermi superfluids to be discovered only in the mid-1980s (high-T_c cuprate superconductors) and mid-2000s (ultracold lithium-6 and potassium-40 fermionic atoms), when strong deviations from BCS behavior were found. But prior to those experimental discoveries, a generalization of the BCS theory was slowly developed to encompass the strong-attraction regime in which fermion pairs become tightly bound diatomic Bose molecules and undergo Bose–Einstein condensation. The key question addressed theoretically was, Are the BCS and BEC theories the endpoints of a more general theory that connects Fermi superfluids to molecular Bose superfluids?

The simplest conceptual and physical picture of the evolution from BCS to BEC superfluidity for *s*-wave pairing can be constructed for low fermion densities and short-ranged interactions, for which the interaction range is much smaller than the average separation between fermions. In that limit the essence of the evolution at zero temperature is reflected in the ratio of the size of fermion pairs to the average separation between the fermions. In the BCS regime, the attraction is weak, the pairs are much larger than their average separation, and they overlap substantially. In the BEC regime, the attraction is strong, the pairs are much smaller than their average separation, and they overlap very little.

Amazingly, a clear picture of the BCS-to-BEC evolution at zero temperature didn't emerge until 1980, when Anthony Leggett realized that the physics could be captured by a simple description in real space of paired fermions with opposite spins.[5] Leggett considered a zero-ranged attractive potential—that is, a contact interaction—between fermions and showed that when the attraction was weak, a BCS superfluid appeared, and when the attraction was strong, a BEC superfluid emerged. Philippe Nozières and Stephan Schmitt-Rink (NSR) used a diagrammatic method with a finite-ranged attraction to extend Leggett's description to temperatures near the critical temperature for superfluidity.[6] Such ideas remained largely academic, however, since the evolution from the BCS to the BEC regime had not materialized in the experimental world.

But the discovery of cuprate high-T_c superconductors in 1986 created a new paradigm for superconductivity. The BCS theory seemed to fail dramatically in some important regions of the phase diagram of cuprate superconductors, some of which have critical temperatures near 100 K. Motivated by the inapplicability of the BCS theory to cuprate superconductors, which seemed to have small electron pairs, Jan Engelbrecht, Mohit Randeria, and I extended the preliminary results of Leggett and NSR as an attempt to understand cuprates.[7] We used a zero-ranged attraction characterized by the experimentally measurable length scale a_s, the so-called scattering length. The natural momentum scale is the Fermi wavenumber k_F, and the strength of the attractive interactions can be described by the dimensionless scattering parameter $1/k_F a_s$. That parameter changes sign in going from weak to strong attraction: The BCS weak-attraction limit is characterized by $1/k_F a_s \ll -1$; the BEC strong-attraction limit, by $1/k_F a_s \gg +1$. The crossover region between the two limits occurs for $-1 < 1/k_F a_s < +1$.

The phase diagram in figure 2 illustrates two important physical concepts of the evolution from BCS to BEC superfluidity. First, the normal state for weak attractions is a Fermi liquid, which evolves smoothly into a molecular Bose liquid. The two regimes are separated by a pair formation (or molecular dissociation) temperature T_{pair} characterized by chemical equilibrium between bound fermion pairs and unbound fermions. Second, T_{pair} and the critical temperature T_c are essentially the same in the BCS limit: Pairs form and develop phase coherence (condense) at the same temperature. But in the BEC limit, fermion pairs (diatomic molecules) form first around T_{pair} and condense at the much lower temperature $T_c = T_{BEC}$, where phase coherence is established.

Two other concepts are shown in figure 2. First is the so-called unitarity limit, where the scattering length diverges. As the scattering parameter $1/k_F a_s$ changes sign from negative to positive, a two-body bound state with characteristic

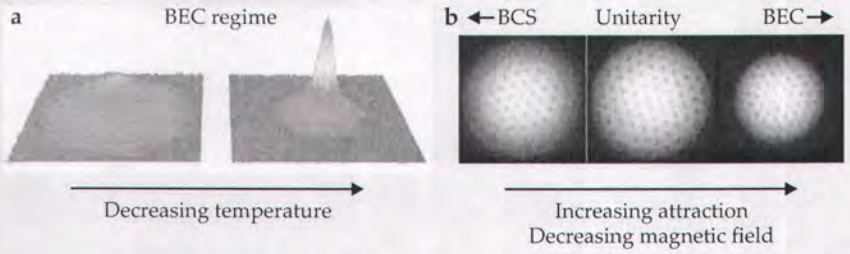

Figure 3. Evidence of superfluidity. (a) Two maps of the density of potassium-40 in the regime where the atoms form small fermion pairs, or molecular bosons. On the left, the temperature is above the critical temperature and the molecules are uncondensed. On the right, the temperature is below the critical temperature and the molecules undergo Bose–Einstein condensation, as evidenced by the sharp peak. (Adapted from ref. 10.) (b) More striking evidence for superfluidity, here of lithium-6. Absorption images taken in the crossover stable region between the Bardeen-Cooper-Schrieffer and BEC regimes (see figure 2) reveal the existence of a lattice of vortices. (Adapted from ref. 11.)

size equal to the scattering length emerges in vacuum (see the box on page 47). Yet despite the vanishing of the scattering parameter and the emergence of a molecular bound state, nothing really dramatic happens to the superfluid state at unitarity. What is more relevant from a many-body perspective is the vanishing of the chemical potential ($\mu = 0$), which occurs beyond the unitarity limit at zero temperature. That special point is the de facto separation between the BCS region, where the energy gap in the elementary excitation spectrum is related to the order parameter and occurs at finite momentum, and the BEC region, where the energy gap occurs at zero momentum and is related to both the chemical potential and the order parameter. It is the qualitative change in the elementary excitation spectrum at zero chemical potential—not the emergence of a bound state in vacuum at the unitarity limit, where the scattering length diverges—that separates the BCS region from the BEC region at zero temperature. But that raises the question, Is it possible to tune the interactions to cross the line of zero chemical potential and go from one region to the other?

Tuning the interactions

In superconductors some tunability of the fermion density can be achieved through chemical doping or electrostatic gating in the same material, and in liquid ^{3}He some change in density is possible under pressure, but essentially no control over interactions is possible. In nuclei and neutron stars, the situation is even worse—there is no control at all over the density or interaction strength. But five years ago, the tuning of interactions became possible in ultracold Fermi atoms through magnetically driven Feshbach resonances (see the box and also Dan Kleppner's column, PHYSICS TODAY, August 2004, page 12). It is this ability that makes ultracold atoms a special laboratory to study strongly correlated fermion systems.

In late 2003, almost simultaneously, three experimental groups succeeded in producing BEC of bound fermion molecules in optical traps at ultracold temperatures. Two groups, Rudolf Grimm's at the University of Innsbruck[8] and Wolfgang Ketterle's at MIT,[9] used ^{6}Li atoms, and a third group, Deborah Jin's at JILA,[10] used ^{40}K. Absorption images of the atoms after they were released from the trap showed a sharp central peak in the density (figure 3a), an important signature of the condensation of molecular bosons (that is, tightly paired fermions). But the true evidence for superfluidity was the experimental detection by the MIT group[11] of a vortex lattice in ^{6}Li when the cloud of trapped fermions was first rotated and then allowed to expand (see figure 3b). Vortices are stable topological excitations that are formed due to circulating superfluid currents and carry one unit of angular momentum. The vortices interact repulsively to form a triangular lattice that is preserved even upon expansion of the cloud since the topological excitations are quite stable.

Additional experimental developments at MIT[12] and Rice University[13] in 2005 initiated the study of Fermi systems (^{6}Li) with population imbalance—that is, having unequal numbers of fermions in distinct hyperfine states, labeled "up" and "down." Starting from an equal population mixture, appropriate application of RF pulses can arbitrarily change the relative populations by converting up fermions to down and vice versa. The ability to control the population of fermions and create imbalances varying almost continuously from equal mixtures to only one occupied state has stimulated substantial experimental and theoretical work to understand phase diagrams throughout the evolution from BCS to BEC superfluidity at zero and finite temperatures.

One expects a minimum of three phases when the population imbalance is fixed and the interaction is changed. As the interaction increases at zero temperature, the system is first a normal, unpaired fluid. It then separates into distinct regions, one containing a paired superfluid and the other containing excess unpaired fermions, before it finally reaches a phase in which the superfluid and excess fermions coexist (see figure 4). A key feature of the phases is that they are perfectly symmetric with respect to population imbalance, and it does not matter if the excess fermions are up or down, since atoms have the same mass.

The next frontiers

The unprecedented control and tunability in ultracold fermions may illuminate the physics of strongly correlated fermions in standard condensed-matter physics, nuclear physics, and astrophysics, where control is much more limited or nonexistent. Among the many possible experimental and theoretical directions, five are perhaps of the most immediate nature.

▶ **Mixtures of fermions of unequal masses.** New possibilities arise when one considers mixtures of fermions of unequal masses, such as ^{6}Li and ^{40}K, ^{6}Li and ^{87}Sr, or ^{40}K and ^{87}Sr. Studying such mixtures is significant not only for atomic physics, but also for condensed-matter physics, where they could simulate fermions with different effective masses, and for quantum chromodynamics (QCD), where they could simulate mixtures of quarks with unequal masses. As in the case of equal masses, a minimum of three phases (normal, phase-separated, and coexisting) is expected for unequal masses throughout the evolution from BCS to BEC superfluidity. However, there is a dramatic asymmetry in the phase diagram of population imbalance versus interaction parameter.

Conceptually, the easiest limit to understand is the BEC regime of a mixture of equal numbers of up and down fermions. If their masses are different, they form heteronuclear diatomic molecules that repel each other weakly and produce a molecular BEC. When excess fermions are present, the paired fermions also repel the excess fermions, but the re-

pulsion is smaller when lighter fermions are in excess, and larger when heavier fermions are in excess, which makes the coexistence region between pairs and lighter excess fermions larger than that of pairs and heavier excess fermions. That asymmetry awaits experimental confirmation, but two major experimental advances are narrowing the gap with theory: Quantum degenerate mixtures of ^{6}Li and ^{40}K have been created experimentally,[14] and Feshbach resonances that permit the control of interactions in such mixtures have been reported.[15]

► **BCS-to-BEC evolution for higher angular-momentum pairing.** Although the evolution from BCS to BEC superfluidity for *s*-wave pairing is fairly well understood theoretically and experimentally, there is no experimental realization of the phenomenon for *p*-wave pairing. Even though *p*-wave pairing has been extensively studied in connection with superfluid liquid ^{3}He, some superconductors, and even neutron stars, most theoretical work has built on the BCS theory, under the assumption that the systems are somewhat weakly interacting. However, ultracold fermions like ^{6}Li and ^{40}K have some known *p*-wave Feshbach resonances between atoms in identical hyperfine states, and those may allow the tuning of *p*-wave interactions.

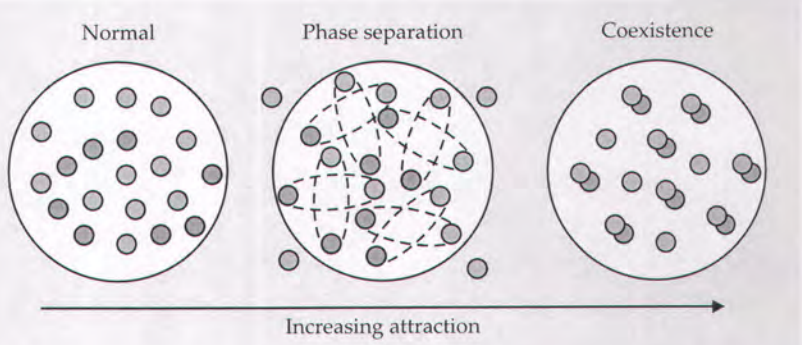

Figure 4. Population imbalances, which can be created by applying RF pulses, can affect the superfluid state as it evolves from the Bardeen-Cooper-Schrieffer to the Bose–Einstein condensation regime. Some of the possible phases at zero temperature are illustrated here for an excess of "up" (blue) atoms. For a fixed and sufficiently large population imbalance the ground state of the system with weak attraction between the fermions is a normal mixture of unpaired "up" and "down" (red) atoms—they cannot overcome a pairing barrier created by their population imbalance. As the attraction increases, the blue and red atoms acquire enough energy to pair with each other but repel the excess atoms, which leads to phase separation between the superfluid's paired fermions and excess, unpaired fermions. As the attraction between fermions is increased further, the pairs become more tightly bound and repel the excess atoms less; the result is a mixed state of coexisting superfluid and excess fermions.

Although *p*-wave resonances are typically much narrower than *s*-wave and are much more difficult to study, they possess much richer physics due to their anisotropy. A simple conceptual example of that richness is the presence of an anisotropic elementary excitation spectrum that is gapless in the BCS regime but becomes fully gapped in the BEC regime. That evolution represents a phase change that is not accompanied by a change in the order-parameter symmetry (*p*-wave in both regimes), and thus it cannot be fully described by current theories of phase transitions. An experimental observation of the phenomenon would be a textbook example of the need for a new, generalized theory.

► **Effects of disorder in BCS-to-BEC evolution.** Although disorder is difficult to control in standard condensed-matter systems, random potentials for trapped ultracold fermions can be produced under controlled circumstances. That allows the study of the effects of weak and strong disorder throughout the evolution from BCS to BEC superfluidity and the study of three-dimensional phase diagrams involving temperature, interaction, and disorder.

To give a sense of how rich that phase diagram can be, consider first a random potential that is independent of the hyperfine state of the atoms. Such a potential corresponds to the case of nonmagnetic impurities in standard condensed-matter systems. For an *s*-wave BCS superfluid, the amplitude and phase of the order parameter are strongly coupled, such that the breaking of Cooper pairs and destruction of phase coherence occur simultaneously. Because the random potential is not pair-breaking, it does not affect the phase coherence associated with the order parameter, and thus the critical temperature in the presence of weak disorder is essentially unchanged. The robustness of *s*-wave BCS superfluids with time-reversed fermion pairing (for example, pairs with opposite momenta and spin) in the presence of weak disorder was proposed nearly 50 years ago by Philip Anderson and is known as Anderson's theorem. For weakly disordered BEC superfluids, in contrast, the breaking of local pairs and the loss of phase coherence occur at very different energy scales. The critical temperature is strongly affected by weak disorder, since phase coherence is more easily destroyed without the need to break local pairs simultaneously, and Anderson's theorem doesn't apply.

One can also study the phase diagram for *s*-wave superfluids in random potentials that are dependent on the hyperfine state of the atoms; such potentials simulate the effects of magnetic impurities in standard condensed matter. The effects of weak disorder in the BCS regime in this case are substantial, since the random potential is pair-breaking, which leads to the loss of phase coherence and to a quick suppression of T_c. The T_c reduction in the BEC regime is also strong, as with state-independent random potentials, since phase coherence is again quickly destroyed without pair breaking. However, the effects of strong disorder on superfluidity are more complex, thanks to disorder-induced localization—termed Anderson localization—of fermions in the normal state of the BCS regime and of bosons in the normal state of the BEC regime. The understanding of the normal and superfluid states in the strong-disorder limit throughout the evolution from BCS to BEC is still a theoretical challenge, but experimentalists may be able to reach that exciting regime in a controlled way and to study disorder-induced phase transitions.

► **Mixtures of fermions with three hyperfine states.** Expanding the number of hyperfine states from two to three, which can be labeled red, blue, and green (or 1, 2, and 3), opens quite interesting possibilities, as there can be three types of *s*-wave pairings: red–blue, blue–green, and green–red. Such pairs may form a color superfluid with the coexistence of the three types of superfluids. That is analogous to a situation encountered in QCD in which quarks may pair in different color states in the cores of neutron stars and produce a color

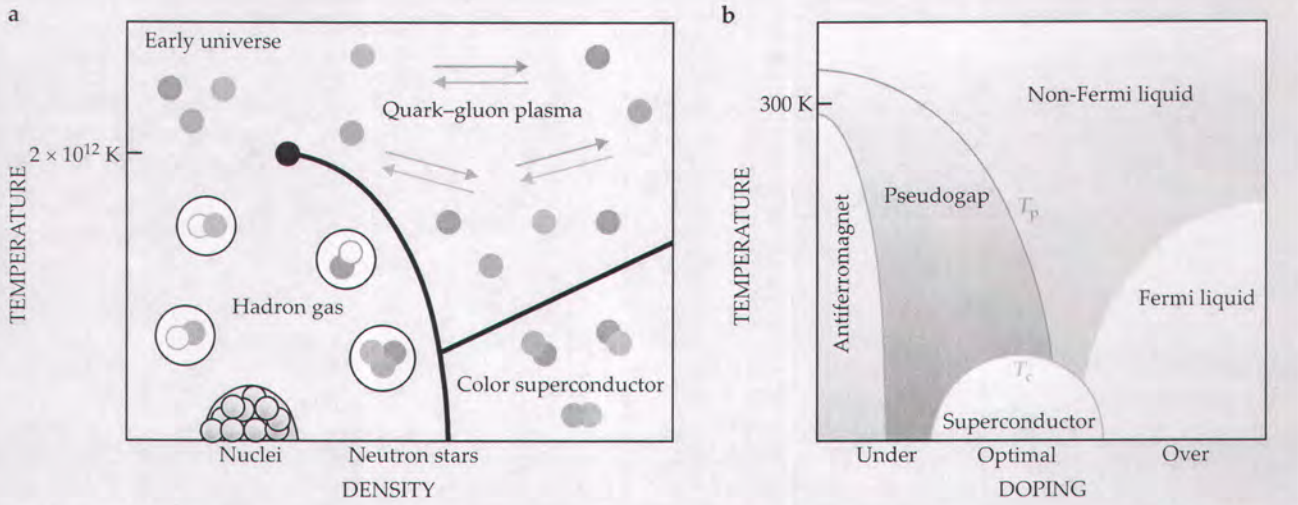

Figure 5. Simulating other systems. The ability to control interactions among ultracold fermions allows connections to be made with other areas of physics and may help address some of the key issues involving strongly correlated fermions in neutron stars, nuclei, and condensed matter. **(a)** Quarks of color quantum states red, blue, and green may pair at "low" temperatures and high densities, producing a color superconductor in the core of a neutron star. Color superconductivity might be simulated in ultracold Fermi atoms if a stable mixture of three hyperfine states for the same type of atom can be produced. **(b)** Cuprate superconductors, which have this complicated phase diagram, might be simulated by ultracold fermions in optical lattices. Although the temperature scales and the densities for ultracold atoms are much smaller than the corresponding temperatures and densities for color or cuprate superconductors, the ratios of the temperature to the Fermi temperature may be close, permitting some parallels to be drawn. It would be remarkable to achieve color superconductivity without quarks, and high-temperature superconductivity in a lattice without copper and oxygen.

superconductor at densities several times larger than those found in typical nuclear matter (see figure 5a).

Important differences exist, however, between the color superconductor expected in QCD and the color superfluid expected in ultracold fermions. First, ultracold atoms are neutral and quarks are fractionally charged particles. Second, the densities of ultracold fermions are extremely low, while the densities for quarks are extremely high. Third, whereas quarks have a threefold degeneracy of their color, the degeneracy of hyperfine states in ultracold atoms is usually lifted by an external magnetic field. The need to control two-body collisions and prevent three-body collisions of trapped atoms involving three distinct hyperfine states makes experiments difficult, and color superfluidity has not yet materialized in ultracold fermions. Still, it is not crazy to think about it! A natural candidate for color superfluidity is ^{6}Li, which has three hyperfine states that might be suitable, if losses can be cleverly controlled. Other ultracold fermions, including Fermi isotopes of ytterbium, are on the horizon. Furthermore, there is the promise of being able to control the interactions and populations of ultracold atoms to obtain and explore phases that do not yet have analogous behavior in QCD.

► **Ultracold fermions in optical lattices.** The evolution from BCS to BEC superfluidity for *s*-wave systems in 3D cubic lattices was first discussed by NSR in 1985, but experiments probing superfluidity of ultracold fermions in optical lattices are just beginning. Tilman Esslinger and colleagues at ETH Zürich reported the production of ^{40}K molecules in 3D cubic optical lattices using *s*-wave Feshbach resonances in early 2006,[16] but no evidence of a superfluid state was found until later that year, when Ketterle and coworkers loaded ^{6}Li atoms in optical lattices and their pairs formed a condensate.[17] Those two experiments opened the door to studies of superfluid-to-insulator transitions in optical lattices and are likely to stimulate and renew the interest on the possible realization of *d*-wave superfluidity in nearly 2D lattices like those encountered in the high-T_c cuprate superconductors, which have a complex phase diagram (see figure 5b) and are known to be *d*-wave superconductors. It would be quite interesting to tune interactions and filling factors of ultracold fermions in optical lattices, and try to reproduce the phase diagram of cuprate superconductors.

Predicting the future

The unprecedented control over interactions in various dimensionalities and geometries has put research of ultracold fermions in harmonic traps and optical lattices at the forefront of investigations into the behavior of Fermi condensates and strongly interacting fermions. In particular, exotic phases of QCD, like color superconductivity, and superfluid phases in neutron stars and nuclear matter may have analogous counterparts in tabletop experiments involving ultracold fermions. Furthermore, studies of disorder-induced phenomena are also within experimental reach, and insights into *p*- and *d*-wave superconductivity found in condensed-matter physics are just around the corner, as ultracold fermions loaded into optical lattices begin to be explored. No one has a crystal ball to predict the future, but research on ultracold atoms will likely provide insight into the simulation and understanding of many known and unknown phases of nuclear, atomic, molecular, and condensed-matter physics.

I thank Sam Bader, Ian Spielman, Kris Helmerson, and Steve Anlage, among other colleagues, for reading this manuscript at various stages of its production and for their valuable suggestions. This article is dedicated to my father and mother, who passed away during its writing.

References

1. F. London, *Nature* **141**, 643 (1938); *Phys. Rev.* **54**, 947 (1938).
2. A. Einstein, *Preuss. Akad. Wiss. Berlin Ber.* **22**, 261 (1924); **23**, 3 (1925); S. N. Bose, *Z. Phys.* **26**, 178 (1924).
3. J. Bardeen, L. N. Cooper, J. R. Schrieffer, *Phys. Rev.* **106**, 162 (1957); **108**, 1175 (1957).
4. M. R. Schafroth, S. T. Butler, J. M. Blatt, *Helv. Phys. Acta* **30**, 93 (1957).
5. A. J. Leggett, *J. Phys. Colloq.* **41**, 7 (1980).
6. P. Nozières, S. Schmitt-Rink, *J. Low Temp. Phys.* **59**, 195 (1985).
7. C. A. R. Sá de Melo, M. Randeria, J. R. Engelbrecht, *Phys. Rev. Lett.* **71**, 3202 (1993).
8. S. Jochim, M. Bartenstein, A. Altmeyer, G. Hendl, S. Riedl, C. Chin, J. Hecker Denschlag, R. Grimm, *Science* **302**, 2101 (2003).
9. M. W. Zwierlein, C. A. Stan, C. H. Schunck, S. M. F. Raupach, S. Gupta, Z. Hadzibabic, W. Ketterle, *Phys. Rev. Lett.* **91**, 250401 (2003).
10. M. Greiner, C. A. Regal, D. S. Jin, *Nature* **426**, 537 (2003).
11. M. W. Zwierlein, J. R. Abo-Shaeer, A. Schirotzek, C. H. Schunck, W. Ketterle, *Nature* **435**, 1047 (2005).
12. M. W. Zwierlein, A. Schirotzek, C. H. Schunck, W. Ketterle, *Science* **311**, 492 (2005).
13. G. B. Partridge, W. Li, R. I. Kamar, Y. Liao, R. G. Hulet, *Science* **311**, 503 (2006).
14. M. Taglieber, A. C. Voigt, T. Aoki, T. W. Hänsch, K. Dieckmann, *Phys. Rev. Lett.* **100**, 010401 (2008).
15. E. Wille, F. M. Spiegelhalder, G. Kerner, D. Naik, A. Trenkwalder, G. Hendl, F. Schreck, R. Grimm, T. G. Tiecke, J. T. M. Walraven, S. J. J. M. F. Kokkelmans, E. Tiesinga, P. S. Julienne, *Phys. Rev. Lett.* **100**, 053201 (2008).
16. T. Stöferle, H. Moritz, K. Günter, M. Kühl, T. Esslinger, *Phys. Rev. Lett.* **96**, 030401 (2006).
17. J. K. Chin, D. E. Miller, Y. Liu, C. Stan, W. Setiawan, C. Sanner, K. Xu, W. Ketterle, *Nature* **443**, 961 (2006). ■

PLASMA
CHARACTERIZATION

EQP mass and energy analyzers measure key plasma parameters providing the detailed information you need to understand your plasma:

- ion mass and energy analysis
- RF, DC, ECR & pulsed plasma
- neutrals & neutral radicals

4. EQP

Quantify your plasma: ion mass and energy, ion and neutral density, radicals by TIMS and EAMS, integrated timing circuitry for time resolved work

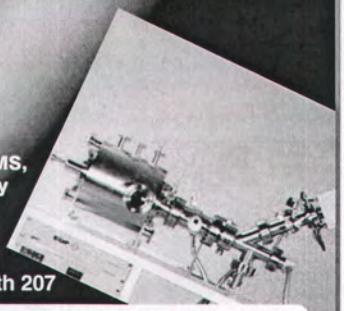

See Hiden at AVS — booth 207

HIDEN ANALYTICAL

for further details of Hiden Analytical products contact:
info@hideninc.com
www.HidenInc.com

Quadrupoles for advanced science

See www.pt.ims.ca/16305-24

NanoTracker™

Ultimate 3D Particle Tracking and Optical Tweezers Platform. Quantify Forces in NanoBiology.

Trap, track and manipulate nanoparticles.
Observe cell/particle interactions in real time and 3D.
Measure forces between single-molecules.
JPK NanoTracker™ – a new class of instrumentation.

www.jpk.com

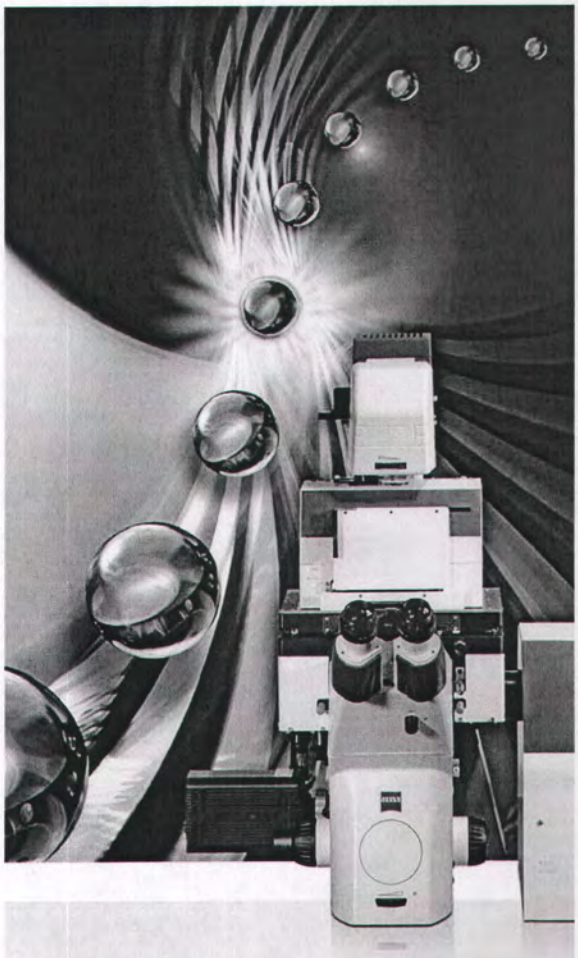

JPK Instruments

Nanotechnology for Life Science

See www.pt.ims.ca/16305-25

Preparing a highly degenerate Fermi gas in an optical lattice

J. R. Williams, J. H. Huckans, R. W. Stites, E. L. Hazlett, and K. M. O'Hara*
Department of Physics, Pennsylvania State University, University Park, Pennsylvania 16802-6300, USA
(Dated: November 6, 2008)

We propose a method to prepare a sample of fermionic atoms in a three-dimensional (3D) optical lattice at unprecedentedly low temperatures and uniform filling factors. The process involves adiabatic loading of atoms into multiple energy bands of an optical lattice followed by a filtering stage whereby atoms from all but the ground band are removed. Of critical importance is the use of a non-harmonic trapping potential, taken here to be the radial profile of a high-order Laguerre-Gaussian laser beam, to provide external confinement for the atoms. For realistic experimental parameters, this procedure should produce samples with temperatures $\sim 10^{-3}$ of the Fermi temperature. This would allow the investigation of the low-temperature phase diagram of the Fermi-Hubbard model as well as the initialization of a high-fidelity quantum register.

PACS numbers: 03.75.Ss, 32.80.Pj, 03.67.Lx, 37.10.De, 37.10.Jk, 05.30.-d

Investigations of degenerate Fermi gasses loaded into optical lattices have indicated that these systems are ideal for creating a robust quantum register for quantum computing applications [1, 2] as well as providing a testing ground for paradigm models of condensed matter physics. Models currently under investigation include studying Fermi surfaces and band insulator states [3], fermionic superfluidity in a lattice [4], and transport properties of interacting fermions in one and three dimensional optical lattices [5, 6]. These seminal experiments demonstrate the high precision and versatility available in simulating solid state systems with fermions in optical lattices.

Theoretical studies of such systems have predicted that a number of exotic phases emerge at low temperatures, including quantum magnetic ordering and possibly d-wave superfluidity [7, 8]. However, temperatures low enough to observe exotic phases such as these are difficult to achieve when optical lattices are loaded with a harmonic external confining potential. It has been theoretically predicted [9] and experimentally observed [3] that fermions adiabatically loaded into an optical lattice with harmonic external confinement experience heating for all but very high initial temperatures and filling factors (number of atoms per lattice site) [10].

Alternative methods to prepare fermionic atoms in optical lattices at low temperatures and/or high uniform filling factors include: cooling by adiabatic loading into a three-dimensional (3D) homogeneous trapping potential with high filling factor [11], defect filtering in a state dependent optical lattice [1], adiabatic loading [2] and filtering [12] of high entropy atoms from a 1D lattice with harmonic confinement.

In this Letter, we propose a method to prepare a highly degenerate Fermi gas in a 3D optical lattice using a box-like potential for external confinement and taking advantage of the Pauli exclusion principle to selectively remove atoms from multiply-occupied lattice sites. Specifically, we assume that the radial profile of a blue-detuned, high-order Laguerre-Gaussian (LG) laser beam provides confinement along each cartesian axis. The atoms are prepared via a two step process: (1) adiabatically loading atoms initially confined in the LG trap into a superimposed optical lattice, followed by (2) irreversibly filtering atoms from all but the ground energy band (see Fig. 1). We find that when the Fermi energy of the system is sufficiently large, such that atoms begin to significantly populate the second energy band prior to filtering, considerable cooling is achieved; whereas for lower filling factors heating is observed.

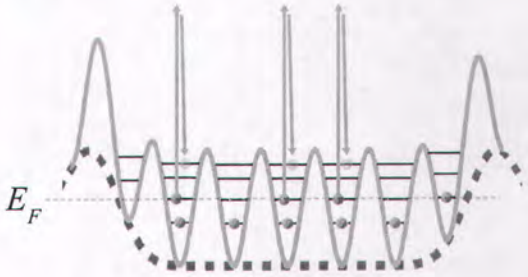

FIG. 1: (color online) We filter high entropy atoms from a combined box-like potential (blue dashed line) and optical lattice (red solid line) by selectively removing atoms from all but the ground energy band. Amplitude modulation of the lattice potential can selectively transfer these atoms to high-lying bands via a two-photon transition where they then tunnel out of the region. Dramatic cooling results when the Fermi energy (prior to filtering) lies within the second band.

The energy spectrum of a system of ultracold atoms is greatly affected by the addition of a 3D cubic optical lattice which can be formed by three perpendicular sets of retroflected Gaussian laser beams detuned far from resonance. In a homogeneous trapping potential, the lattice breaks the translational symmetry of the system, resulting in a series of discrete energy bands whose width and energy spacings are dependent on the intensity and wavelength of the laser light (see Fig. 2(a)). Bezett and

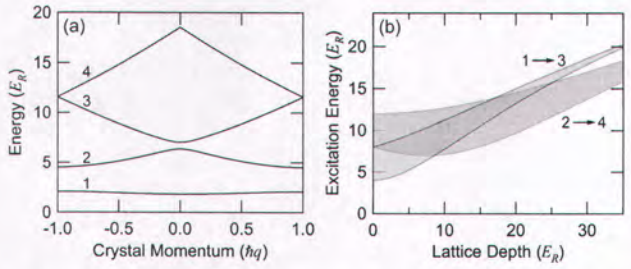

FIG. 2: (color online) (a) Band structure for a $5\,E_R$ deep lattice. (b) Atoms can be selectively excited from the n to $n+2$ energy band by modulating the amplitude of the optical lattice light. The excitation energy between bands 1 and 3 (blue) and 2 and 4 (red) for fermions in all crystal momenta states are shown. As the depth of the optical lattice approaches $35\,E_R$, the excitation energy bands separate, thereby demonstrating the feasibility of performing the band selective excitations required in our filtering method.

Blakie demonstrated that this energy band structure can be exploited to dramatically increase the degeneracy of the sample for a homogeneous system [11]. For a dense atomic gas, with a filling factor greater than unity, application of the lattice increases the Fermi energy, since it lies within the first excited band, and compresses the Fermi surface resulting in a dramatic reduction in the degeneracy temperature T/T_F, where T_F is the Fermi temperature.

This band structure also permits state-selective operations to manipulate and probe the energy distribution of the sample. One such method involves modulating the depth of the optical lattice to selectively excite atoms from the n to $n+2$ energy band with no change in the crystal momentum q [13]. In contrast to non-interacting Bose systems, where a single q can be macroscopically occupied, a Fermi system necessarily begins to fill the bottom band and $\Delta q = 0$ transitions must be excited for all occupied values of q. In Fig. 2(b), we show band excitation energies as a function of lattice depth for $n = 1 \rightarrow 3$ and $n = 2 \rightarrow 4$ transitions spanning all q within a Brillouin zone. By loading the sample into an optical lattice with a depth of $V_0 = 35\,E_R$ (where $E_R = \hbar^2 k^2/2m$ is the recoil energy and k is the wavenumber of the laser light), we find that these transitions are well resolved. It is therefore possible to apply a filtering process which selectively removes atoms from all but the ground energy band. Using adiabatic rapid passage, population may be selectively transferred from $n = 2 \rightarrow 4$ by sweeping the amplitude modulation frequency from below to above all $2 \rightarrow 4$ transition frequencies while remaining below the lowest $1 \rightarrow 3$ transition frequency. Then, lowering the height of the trapping potential allows atoms in the third and higher energy bands to tunnel out of the system.

In order to experimentally approximate the homogenous lattice potential described above, we consider the addition of a box-like external potential produced by a blue-detuned, ℓ^{th}-order, LG laser beam with a radial profile

$$V_{\rm LG}(r) \;=\; V_{\rm peak}\left(\frac{2\,e\,r^2}{w_0^2\,\ell}\right)^{\ell} e^{-2r^2/w_0^2} \qquad (1)$$

at the beam waist w_0. For a given charge ℓ, the peak value $V_{\rm peak}$ of the potential occurs at $r_{\rm max} = w_0\sqrt{\ell/2}$ and the width of this peak decreases with decreasing w_0. Therefore, for a given trap size $r_{\rm max}$, the LG profile more closely approximates a box potential when w_0 is reduced and ℓ is correspondingly increased. Trapping of ultracold gases has been demonstrated in single or crossed beam configurations of LG beams up to $\ell = 16$ [14–16].

Along a given cartesian axis, we take the single particle Hamiltonian to be

$$H(x) \;=\; \frac{-\hbar^2}{2m}\frac{\partial^2}{\partial x^2} + V_{\rm LG}(x) \qquad (2)$$
$$+V_0\cos^2(kx+\phi_x) + \frac{1}{2}m\omega^2 x^2,$$

where the third term represents a lattice potential of depth V_0 and phase offset ϕ_x. We also include a harmonic term that arises if red-detuned Gaussian beams are used to produce the lattice potential; in this case $\omega \propto \sqrt{V_0}$. The 1D eigenvalues and eigenfunctions for a given depth of the optical lattice are calculated by numerically diagonalizing the Hamiltonian (Eq. 2) using the method described in [17]. For sufficiently shallow lattice depths, the low energy eigenstates are delocalized and closely approximate Bloch states in the first band of a homogeneous system. However, higher energy states are either localized at the edges of the trap (i.e. near $x = r_{\rm max}$) or delocalized and correspond to Bloch states in higher bands. While a band structure picture is not strictly valid for this inhomogeneous system, we classify the set of eigenfunctions without nodes to constitute the first band, $\epsilon_{1{\rm band},n}$.

We extend this model to three dimensions by assuming a separable Hamiltonian $H_{\rm 3D} = H(x) + H(y) + H(z)$. For simplicity, we assume equal lattice depths in each direction. The 3D spectrum ($\mathcal{E}_m$) for a given depth of the optical lattice is then generated by calculating all possible combinations of the sum $\mathcal{E}_m = \epsilon_i + \epsilon_j + \epsilon_k$ for all values of the 1D eigenenergies (ϵ_p) in each spatial direction. The 3D energy spectrum for energy states in the first band of the optical lattice is calculated in a similar manner ($\mathcal{E}_{1{\rm band},m} = \epsilon_{1{\rm band},i} + \epsilon_{1{\rm band},j} + \epsilon_{1{\rm band},k}$).

In calculating thermodynamic quantities during the proposed cooling method, we assume constant thermal equilibrium before and after the selective removal of atoms from high-lying bands. Equilibrium is maintained by elastic collisions in a 50/50 mixture of spin-1/2 fermions and changes in the trapping potential are adiabatic with respect to the rethermalization time scale.

However, we also assume that the interactions are weak enough to not significantly modify the single-particle energy spectrum, $\mathcal{E}_m$. We therefore use $\mathcal{E}_m$ when calculating the following quantities:

$$\begin{aligned} N &= 2\sum_m \frac{1}{1+\exp[(\mathcal{E}_m-\mu)/k_BT]}, \\ E &= 2\sum_m \frac{\mathcal{E}_m}{1+\exp[(\mathcal{E}_m-\mu)/k_BT]}, \\ \frac{S}{k_B} &= 2\sum_m \ln[1+\exp[(\mathcal{E}_m-\mu)/k_BT]] + \frac{E}{k_BT} - \frac{\mu}{k_BT}N, \end{aligned} \tag{3}$$

where T is the temperature, μ is the chemical potential of an atom in either spin state, N is the total number of atoms, E is the total energy in the system, and S is the total entropy. The degeneracy temperature is given by T/T_F where $k_BT_F = \mathcal{E}_N$, the energy of the N^{th} eigenstate of the multi-band, 3D spectrum. After filtering, the thermodynamic quantities in Eq. 3 are calculated for atoms only in the first band using $\mathcal{E}_{1\text{band},m}$.

Our proposed method for cooling the atoms is comprised of (1) an adiabatic increase in the lattice depth starting from zero, (2) a non-adiabatic selective filtering of atoms and (3) an optional adiabatic change to a final lattice depth. To calculate changes in thermodynamic quantities during these stages we use the following procedures. For adiabatic changes of the potential we (1) calculate S for a given N and initial temperature T_i using the energy spectrum for the initial potential and (2) numerically solve for μ_f and the final temperature T_f in Eq. 3 using the spectrum for the final potential, assuming N and S are conserved. In contrast, for the selective filtering stage we (1) start from a thermalized sample of N_i atoms at temperature T_i for a given spectrum, (2) calculate, given this distribution, the energy E_f and number N_f for atoms *restricted to the first band*, and (3) solve for μ_f and the temperature T_f in Eq. 3 using the multi-band energy spectrum assuming the sample equilibrates with total energy E_f and number N_f.

We consider a 50/50 spin mixture of ^{6}Li atoms initially trapped in a LG trapping potential with $\ell = 12$, $V_\mathrm{peak} = 35\,E_R$ and $r_\mathrm{max} = 13.5\,\mu$m. For reasonable lattice beam properties ($k = 2\pi/1064\,$nm and a waist of $200\,\mu$m) we find $\omega = 2\pi\,(586\mathrm{Hz})$ for the final lattice depth $V_{0,\mathrm{f}} = 35\,E_R$. The final degeneracy temperatures after adiabatic loading and filtering, along with the final atom number are shown in Fig. 3 for various initial degeneracy temperatures and sample sizes. In each case $\phi_x = \phi_y = \phi_z = 0$. This data shows that the thermodynamic properties of the system are highly dependent on the initial filling factor and can be separated into two distinct regions A and B. The vertical dashed line which separates the regions represents the number of atoms at which the Fermi energy enters the second band.

In region A, the Fermi energy before filtering lies below the second energy band. For very low filling factors, an increase in T/T_F is observed for all initial temperatures. This increase in T/T_F occurs because T_F decreases more than T as the lattice depth increases. Additionally, Fig. 3(b) demonstrates that we are not significantly filtering atoms for low initial temperatures. As the Fermi energy approaches the second energy band, we see a dramatic decrease in the final T/T_F. In this regime, where atoms are beginning to significantly occupy the localized energy states at the edge of the trapping potential, a dramatic increase of the Fermi energy is observed.

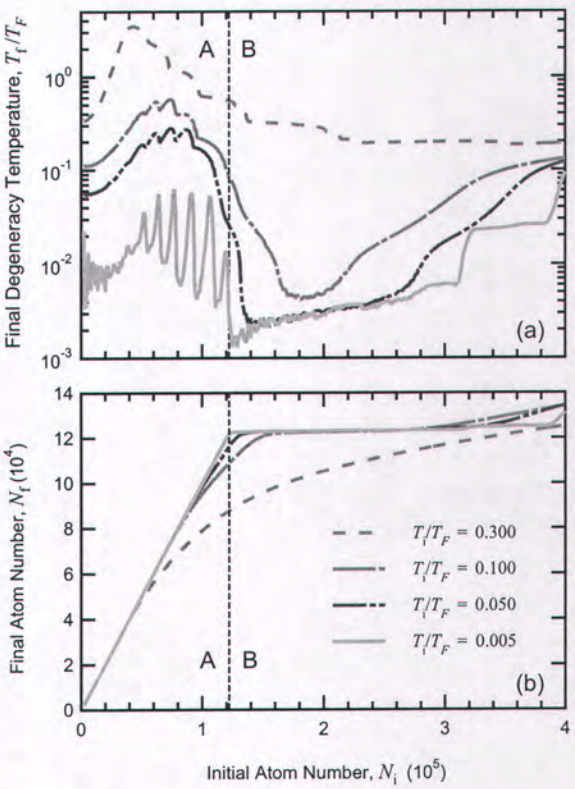

FIG. 3: (color online) As a function of initial atom number we report (a) the final degeneracy temperature and (b) the final atom number after implementing the proposed cooling and filtering procedure for various initial temperatures between 0.005 and $0.3\,T_F$. The vertical dashed line represents the number of atoms for which the Fermi energy enters the second band. The trap and lattice parameters are as described in the text.

In region B, the density is such that the Fermi energy before filtering lies within the second band. In this region the adiabatic increase of the lattice depth results in a dramatic increase in T_F, a substantial reduction in the temperature T [11], and allows for a significant reduction in entropy during the filtering stage. We find that significant cooling is achieved for initial temperatures in the vicinity of $T_\mathrm{i} = 0.1\,T_F$. Above this initial temperature cooling is less efficient. Below this initial tempera-

ture, the final T/T_F after filtering saturates. As can be seen in Fig. 3(b), N_f is extremely insensitive to fluctuations in N_i for low initial temperatures. For example, at $T_\mathrm{i} = 0.05\,T_F$, a variation of $\pm 10\%$ around $N_\mathrm{i} = 1.6 \times 10^5$ yields a variation of only $+0.09\%/-0.2\%$ in N_f.

The cooling efficiency and number filtering were dependent on the choice of phases ϕ_x, ϕ_y and ϕ_z due to the sensitive effect these phases had on the the location of localized edge state eigenenergies relative to the Fermi energy. To study this effect, we modeled the system allowing the phase in each direction to be independently selected from the set $\phi_\alpha = (0, \pi/10, ..., \pi/2)$. We considered samples with an initial temperature $T_\mathrm{i} = 0.05\,T_F$ and an initial number $N_\mathrm{i} = 1.6 \times 10^5$ atoms, parameters within the saturated regime for all choices of phase and close to optimal for cooling. From the set of all possible phase combinations, we find an average final temperature $T_\mathrm{f} = 0.0031\,T_F$ where 10% of the ensemble achieved temperatures below $T_{10} = 0.0023\,T_F$ and 90% were below $T_{90} = 0.004\,T_F$. From this same set, we find an average final number $N_\mathrm{f} = 1.20 \times 10^5$, with $N_{10} = 1.18 \times 10^5$, and $N_{90} = 1.22 \times 10^5$. The filtering process further results in a substantial reduction in entropy. The initial entropy per atom $s_\mathrm{i} = 0.28\,k_B$ is reduced to an average final value of $s_\mathrm{f} = 0.024\,k_B$, with $s_{10} = 0.014\,k_B$, and $s_{90} = 0.033\,k_B$.

It is in general possible to prepare atoms at a low T/T_F in a *shallow* lattice potential, if so desired, by adiabatically reducing the lattice depth after the filtering stage. Continuing the example from above, when the lattice depth is reduced to $5\,E_R$ we find an average final temperature $T_\mathrm{f} = 0.002\,T_F$, $T_{10} = 0.0013\,T_F$, and $T_{90} = 0.0028\,T_F$.

We now consider the effects of the charge ℓ of the LG beam for samples with an initial $T_\mathrm{i} = 0.05\,T_F$, phase $\phi_x = \phi_y = \phi_z = 0$, final lattice depth of $35\,E_R$, and various initial atom numbers. For each ℓ-value, the waist of the LG beam is adjusted such that the number of states below the second energy band is held constant at 1.22×10^5. As shown in Fig. 4, the cooling efficiency of this procedure is highly dependent on the charge. Note that for $\ell = 1$, which approximates harmonic external confinement, the final degeneracy temperature T_f/T_F never drops below its initial value of $T_\mathrm{i}/T_F = 0.05$. For $\ell \gtrsim 8$, the minimum degeneracy temperature saturates to $T_\mathrm{f}/T_F \lesssim 0.003$. For higher values of ℓ, the extent of the saturation regime grows. We believe that this saturation is caused by localized atoms at the edges of the LG potential rethermalizing into higher energy bands.

In this Letter we proposed a method for preparing a sample of highly degenerate fermions by adiabatic loading into a combined optical lattice and "box-like" trapping potential followed by selective removal of atoms from all but the ground energy band. Numerical calculations for sample sizes $\sim 10^5$ predict that temperatures $\sim 10^{-3}\,T_F$ can be prepared in this manner. This method

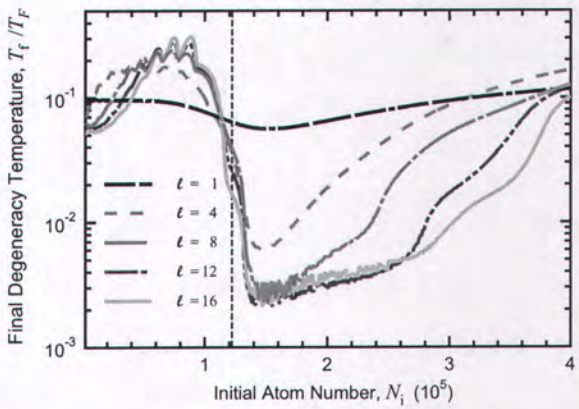

FIG. 4: (color online) The effects of the charge ℓ of the Laguerre - Gaussian trapping potential on the efficiency of our proposed cooling and filtering method. For each data set, the initial temperature $T_\mathrm{i} = 0.05\,T_F$ and the phases $\phi_x = \phi_y = \phi_z = 0$. For all ℓ values, the number of atoms at which the Fermi energy enters the second band (vertical dashed line) is held constant.

is robust against initial number and temperature fluctuations for a sufficiently cold initial sample of atoms and yields samples with little variance in the final number. While the selective removal of atoms must occur in a deep lattice (in order to spectrally resolve the band excitations), subsequent reduction of the lattice depth, if desired, yields a modest amount of additional cooling. We expect that this method can be scaled to larger samples for which still lower degeneracy temperatures would be attained due to the diminished role localized edge states would play. Further, the "box-like" trapping potential offers an ideal spatial profile for simulating solid state physics with degenerate atoms in optical lattices as the relatively flat central region allows for a large number of delocalized states while the curvature at the edges of the traps removes the constraint of loading exact atom numbers to realize insulating states. Atoms prepared in this manner should be sufficiently cold to explore quantum spin phases of fermionic atoms which are currently inaccessible, and could provide a physical realization of an essentially perfect quantum register.

We gratefully acknowledge support from the Air Force Office of Scientific Research (Award No. FA9550-05-1-035112) and the Physics Division of the Army Research Office (Grant No. W911NF-06-1-0398) as well as discussions with David Weiss regarding this work.

* kohara@phys.psu.edu

[1] P. Rabl, A. J. Daley, P. O. Fedichev, J. I. Cirac, and P. Zoller, Phys. Rev. Lett. **91**, 110403 (2003).

[2] L. Viverit, C. Menotti, T. Calarco, and A. Smerzi, Phys. Rev. Lett. **93**, 110401 (2004).
[3] M. Köhl, H. Moritz, T. Stöferle, K. Günter, and T. Esslinger, Phys. Rev. Lett. **94**, 080403 (2005).
[4] J. K. Chin, D. E. Miller, Y. Liu, C. Stan, W. Setiawan, C. Sanner, K. Xu, and W. Ketterle, Nature **443**, 961 (2006).
[5] L. Pezzé, L. Pitaevskii, A. Smerzi, S. Stringari, G. Modugno, E. DeMirandes, F. Ferlaino, H. Ott, G. Roati, and M. Inguscio, Phys. Rev. Lett. **93**, 120401 (2004).
[6] N. Strohmaier, Y. Takasu, K. Günter, R. Jördens, M. Köhl, H. Moritz, and T. Esslinger, Phys. Rev. Lett. **99**, 220601 (2007).
[7] W. Hofstetter, J. I. Cirac, P. Zoller, E. Demler, and M. D. Lukin, Phys. Rev. Lett **89**, 220407 (2002).
[8] D. Jaksch and P. Zoller, Annals of Physics **315**, 52 (2005).
[9] M. Köhl, Phys. Rev. A **73**, 031601(R) (2006).
[10] P. B. Blakie, A. Bezett, and P. Buonsante, Phys. Rev. A **75**, 063609 (2007).
[11] P. B. Blakie and A. Bezett, Phys. Rev. A **71**, 033616 (2005).
[12] M. Popp, J.-J. Garcia-Ripoll, K. G. H. Vollbrecht, and J. I. Cirac, New J. Phys. **8**, 164 (2006).
[13] J. H. Denschlag, J. E. Simsarian, H. Häffner, C. McKenzie, A. Browayes, D. Cho, K. Helmerson, S. L. Rolston, and W. D. Phillips, J. Phys. B:At. Mol. Opt. Phys. **35**, 3095 (2002).
[14] F. K. Fatemi and M. Bashkansky, Opt. Express **15**, 3589 (2007).
[15] D. P. Rhodes, D. M. Gherardi, J. Livesey, D. McGloin, H. Melville, T. Freegarde, and K. Dholakia, J. Mod. Opt **53**, 547 (2006).
[16] F. K. Fatemi and M. Bashkansky, Opt. Express **14**, 1368 (2006).
[17] D. T. Colbert and W. H. Miller, J. Chem. Phys. **96**, 1982 (1992).

Effect of resonant interactions on the stability of a three-state Fermi gas

J. H. Huckans, J. R. Williams, E. L. Hazlett, R. W. Stites, and K. M. O'Hara*
Department of Physics, Pennsylvania State University, University Park, Pennsylvania 16802-6300, USA
(Dated: November 6, 2008)

We investigate the stability of a three spin state mixture of ultracold fermionic ^{6}Li atoms over a range of magnetic fields encompassing three Feshbach resonances. For most field values, we attribute decay of the atomic population to three-body processes involving one atom from each spin state and find that the three-body loss coefficient varies by over four orders of magnitude. We observe high stability when at least two of the three scattering lengths are small, rapid loss near the Feshbach resonances, and two unexpected resonant loss features. At our highest fields, where all pairwise scattering lengths are approaching $a_t = -2140a_0$, we measure a three-body loss coefficient $L_3 \simeq 5 \times 10^{-22}\,\mathrm{cm}^6/\mathrm{s}$ and a trend toward lower decay rates for higher fields indicating that future studies of color superfluidity and trion formation in a SU(3) symmetric Fermi gas may be feasible.

PACS numbers: 67.85.Lm, 34.50.-s, 67.85.-d, 03.75.Ss

Multi-component Fermi gases with tunable interactions are exceptionally well suited to the study of few- and many-body quantum physics. Ultracold two-state Fermi gases near a Feshbach resonance have been used to characterize the crossover from Bardeen-Cooper-Schreiffer (BCS) superfluidity to Bose-Einstein condensation (BEC) of diatomic molecules [1–7]. Further, a normal to superfluid transition and phase separation have been observed in imbalanced two-state spin mixtures [8–12]. The stability of the two-state mixtures against two- and three-body loss processes was critically important to the success of these experiments.

Recently, there has been considerable interest in the study of three-state Fermi gases with tunable interactions [13–25]. Whereas three-body interactions in ultracold two-state Fermi gases are suppressed by the exclusion principle, the addition of a third spin component allows for the study of three-body phenomena such as the Efimov effect in a Fermi system if pairwise interactions are resonantly enhanced [19, 24]. Further, with this additional spin state there may be competition between multiple pairing states and trion formation [13–17, 20–23]. If pairwise interactions are all attractive and of equal magnitude, the system is symmetric under SU(3) transformations and is predicted to exhibit a novel superfluid phase with SU(2) symmetry and an anomolous number of Goldstone modes [15]. This superfluid phase would be a cold atom analog of the color superfluid phase predicted in quantum chromodynamics (QCD) which undergoes a quantum phase transition to a Fermi liquid of trion states (analogous to baryons) as the ratio of the interaction energy to the kinetic energy is adjusted [18].

Future studies of the above phenomena critically depend on the magnitude of two- and three-body loss rates, particularly when two or more scattering lengths are enhanced by scattering resonances. Two- and three-body loss and heating processes, often enhanced near the resonances [26], can impose stringent limits on the maximum achievable phase space density. Further, the unambiguous observation of three-body resonances requires negligible two-body loss [27].

Most investigations of Fermi gases with tunable interactions have focussed on two-state mixtures. A small admixture of a third spin component has been used for thermometry [28] and recently the rapid decay of a three-state Fermi gas near a Feshbach resonance was noted during an investigation of Cooper pair size by radio-frequency (RF) spectroscopy in a two-state Fermi gas [29]. Very recently our group reported measurements of three-body loss in thermal and degenerate three-state Fermi gases over a wide range of magnetic fields [30] and Ottenstein *et al.* independently reported measurements of three-body loss rate coefficients in a degenerate three-state Fermi gas for field values away from any pairwise scattering resonances [31].

In this Letter, we report the first measurements of three-body loss coefficients for a three-state Fermi gas over a range of magnetic fields where pairwise interactions are resonantly enhanced. This enhancement is due to three overlapping interspecies Feshbach resonances and a zero-energy resonance in the ^{6}Li triplet molecular potential. Further, we demonstrate that all two-state mixtures of the three lowest energy hyperfine states of ^{6}Li are stable against two-body loss processes for almost the entire range of field values between 15 and 953 G, making this three-state mixture well suited to studies of three-body physics. We observe a narrow loss feature at 127 G [32] which may be due to a three-body resonance and an additional state-dependent loss feature at 504 G. Finally, we measure the three-body loss rate coefficient at high fields where all three scattering lengths are asymptoting to the triplet scattering length $a_t = -2140a_0$. This measurement and an observed trend toward lower loss at higher fields has important implications for realizing cold atom analogs of color superfluid and baryon phases in QCD.

We study a ^{6}Li Fermi gas with equal populations in the three lowest energy hyperfine states. Figure 1(a) shows

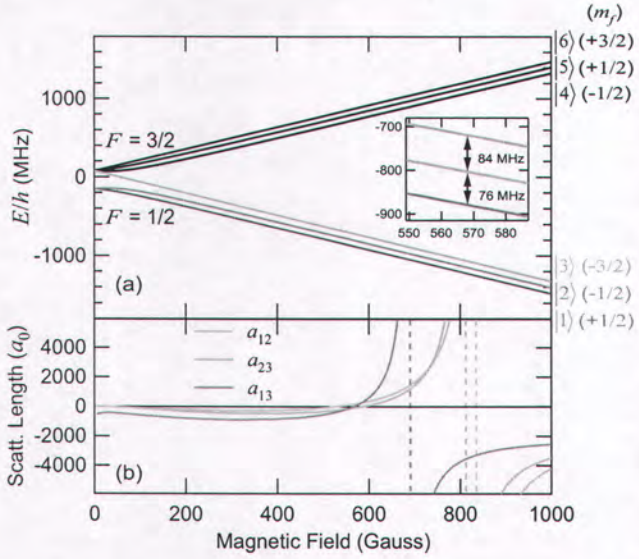

FIG. 1: (color online) (a) Energies of the hyperfine ground states of ^{6}Li in a magnetic field. We create a balanced mixture of the three lowest energy states by applying a RF pulse at a field of 568 G (see inset). (b) The three pairwise s-wave scattering lengths as a function of magnetic field [33] show Feshbach resonances at 690, 811, and 834 G and all asymptote to $a_t = -2140a_0$ at high field.

the energies of the hyperfine ground states of ^{6}Li as a function of magnetic field. At zero field, the three states correspond to $|1\rangle = |\frac{1}{2}, +\frac{1}{2}\rangle$, $|2\rangle = |\frac{1}{2}, -\frac{1}{2}\rangle$ and $|3\rangle = |\frac{3}{2}, -\frac{3}{2}\rangle$ in the $|f, m_f\rangle$ basis. For fields above $\simeq 200$ G, these states become increasingly electron-spin polarized and primarily differ by their nuclear spin projection (i.e. in the $|m_s, m_i\rangle$ basis $|1\rangle \simeq |-\frac{1}{2}, 1\rangle$, $|2\rangle \simeq |-\frac{1}{2}, 0\rangle$ and $|3\rangle \simeq |-\frac{1}{2}, -1\rangle$). The pairwise s-wave scattering lengths between these states (a_{12}, a_{23}, and a_{13}) exhibit three broad overlapping Feshbach resonances as shown in Fig. 1(b) [33]. For very large magnetic fields, each of the pairwise scattering lengths asymptote to the triplet scattering length for ^{6}Li, $a_t = -2140a_0$. Therefore, in the limit of large magnetic fields, this three-state mixture becomes invariant under global SU(3) transformations of the spinor wavefunction.

Two-body spin-flip processes are expected to be especially small for this ultracold ^{6}Li mixture. Spin-exchange collisions become energetically forbidden even in a small magnetic field. Dipolar relaxation is small since (1) the energy released in a spin-flip is not enough to overcome the centrifugal barrier in the d-wave exit channel and (2) electron spin-flip processes are suppressed at high field as the gas becomes increasingly electron-spin polarized in the lowest energy electron spin state.

We can produce a degenerate Fermi gas (DFG) with an equal mixture of atoms in states $|1\rangle$ and $|2\rangle$ once every 5 seconds by evaporatively cooling this mixture in a red-detuned optical dipole trap [34]. During the first second, $\sim 10^8$ ^{6}Li atoms from a Zeeman-slowed atomic beam are collected in a magneto-optical trap (MOT). A crossed optical dipole trap which overlaps the MOT is then turned on and optimally loaded by tuning the MOT laser beams $\simeq 6$ MHz below resonance and reducing their intensity for 7 ms. The atoms are then optically pumped into states $|1\rangle$ and $|2\rangle$ prior to extinguishing the MOT laser beams and field gradient. The two beams which form the optical trap derive from a linearly polarized multi-longitudinal-mode 110 W fiber laser operating at 1064 nm. The beams nearly co-propagate in the vertical direction ($\hat{y}$), have orthogonal polarizations and cross at an angle $\simeq 11°$. The beams are elliptical with calculated e^{-2} waist radii $\sim 30\mu$m and $\sim 100\mu$m at the point of intersection. The maximum trap depth per beam is $\simeq 1$ mK allowing $\sim 5 \times 10^6$ atoms to be initially loaded. We apply a bias field and a noisy RF pulse to create a 50-50 mixture of atoms in states $|1\rangle$ and $|2\rangle$ [34].

Forced evaporation of the atoms occurs at a field of 330 G where the two-state scattering length $a_{12} \simeq -280a_0$. We lower the depth of the optical trap U_0 by a factor of 107 over 3.6 seconds to obtain our final temperature. For the work presented here we study a gas at a temperature $T \gtrsim 0.5\,T_F$ (T_F is the Fermi temperature) so that it is appropriate to treat the cloud as a thermal gas. To suppress further loss by evaporation for the remainder of the experiment, U_0 is then increased by a factor of 4 increasing the ratio of U_0/k_BT by a factor $\simeq 2$. The final oscillation frequencies of the trap are $\nu_x = 3.84$ kHz, $\nu_y = 106$ Hz and $\nu_z = 965$ Hz [35] with a final trap depth per beam $\simeq 40\,\mu$K. The total number of atoms $\simeq 3.6 \times 10^5$ in a balanced two-state mixture at $T \simeq 1.9\,\mu$K for which $T_F \simeq 3.7\mu$K. The background limited $1/e$-lifetime $\simeq 30$ s.

To create an incoherent three-state mixture we first increase the strength of the magnetic field in 10 ms to 568 G where the mixture is stable. We then apply a noisy RF magnetic field with two frequencies centered on the $|1\rangle - |2\rangle$ and $|2\rangle - |3\rangle$ spin-flip transitions, both broadened to a width of 1 MHz by frequency modulation with white noise. A magnetic field gradient of $\simeq 1$ G/cm in the direction of the bias field ($\hat{z}$ direction) is simultaneously applied to dephase the internal state coherence of the sample. The noisy RF field remains on for 50 ms to create an equal mixture of $N \simeq 1.2 \times 10^5$ atoms in each state. At this point, $T = 1.9\,\mu$K with $T_F = 3.2\,\mu$K.

In our first experiment to explore the field dependence of the loss mechanisms in this three-state Fermi gas, we measured the fraction of trapped atoms remaining after an evolution time of 200 ms at fixed magnetic fields between 15 and 953 G. Figure 2(a) shows the fraction remaining for each of the spin states. For each measurement, the magnetic field was ramped in 10 ms from 568 G to the field of interest where it was held constant for either 1 or 201 ms. The field was then ramped in 10 ms to

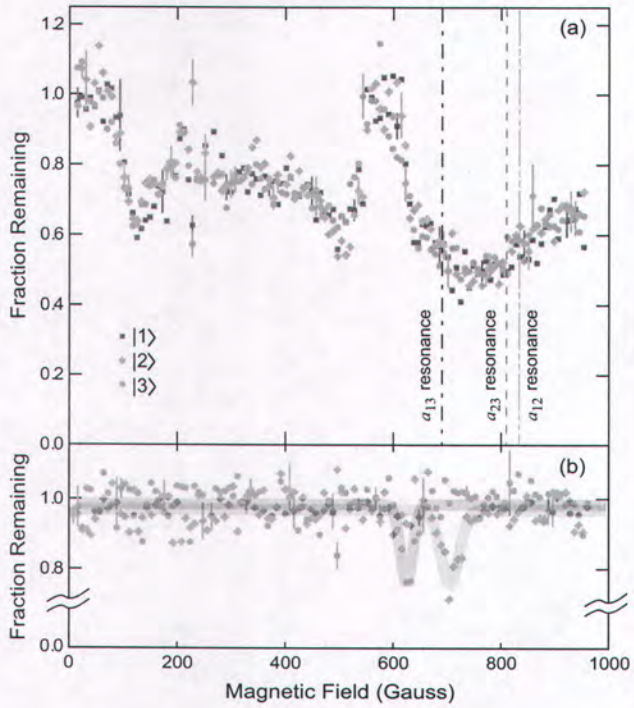

FIG. 2: (color) (a) The fraction of atoms remaining in each of the three spin states after 200 ms of evolution at the magnetic field of interest. (b) Magnetic field dependence of decay in individual two-state mixtures. (•) indicates the fraction remaining in state $|2\rangle$ ($|3\rangle$) of a $|2\rangle - |3\rangle$ ($|1\rangle - |3\rangle$) mixture after 200 ms. The thick lines guide the eye. The representative error bars indicate the standard deviation in the mean.

953 G and held for 20 ms before a 300 μs time-of-flight expansion and absorption imaging at this field. The 10 ms field ramp to 953 G (where $a_{12}, a_{23}, a_{13} < 0$) ensured that any atoms which had formed weakly bound molecules in the vibrational state associated with the Feshbach resonances (but remained trapped) would be disassociated and measured. Further, each of the spin states could be spectroscopically resolved at this field.

To confirm that two-body loss does not contribute significantly to the measurements above, we measured the fraction of atoms remaining after an evolution time of 200 ms at fixed magnetic field values for each of the three possible two-state mixtures. Figure 2(b) shows the fraction remaining in state $|3\rangle$ for a $|1\rangle - |3\rangle$ mixture and state $|2\rangle$ for a $|2\rangle - |3\rangle$ mixture. The fraction of atoms remaining in the $|1\rangle - |2\rangle$ mixture (not shown) is similar to the $|2\rangle - |3\rangle$ data. With the exception of loss features between 600 and 750 G, each mixture was stable. The loss features are due to three-body recombination to bound molecular states associated with the Feshbach resonance. Since the two-state mixtures are stable for fields ≤ 600 G and ≥ 750 G, we can interpret loss features in a three-state mixture at these fields as being due to three-body events involving one atom from each spin state.

In Fig. 2(a), the broad dominant loss feature centered at 720 G occurs in the vicinity of three overlapping interspecies Feshbach resonances. Significant loss due to three-body recombination is expected near these resonances since recombination events involving one atom in each spin state are *not* suppressed by the exclusion principle and one expects a significant increase in the event rate when two or more scattering lengths are resonantly enhanced [36]. Similarly, high stability at zero field and near the zero crossings of the Feshbach resonances is not surprising since at least two of the scattering lengths are small at these fields. At high field where $a_{12}, a_{23}, a_{13} \to a_t$, the stability increases relative to that at 720 G.

Unexpected resonant loss features are observed at 127 and 504 G, where the two-body scattering lengths are not predicted to exhibit any resonances. A possible explanation for the feature at 127 G is that the binding energy of a three-body bound state crosses through zero near this field value. At 504 G, we observe differing degrees of enhanced loss for the three states leading to population imbalance. The feature at 228 G in Fig. 2 is consistent with our estimated location of a $|1\rangle - |3\rangle$ p-wave Feshbach resonance. We also observed a very narrow but inconsistent loss feature at 259 G (not shown).

A second set of experiments measured three-body loss coefficients at fixed magnetic fields where the decaying populations remained balanced. In these experiments, the magnetic field is swept to the field of interest B in 10 ms after creation of the three-state mixture and the number $N(t)$ and temperature $T(t)$ of atoms in state $|3\rangle$ are then measured by time-of-flight absorption imaging at the field B for various delay times t. To extract the three-body loss coefficients, we fit this data assuming one- and three-body loss and heating due to three-body recombination.

When three-body recombination involves one atom from each spin state, the number of trapped atoms in each of the equally populated spin states $N(t)$ evolves according to $\dot{N} = -L_1 N - L_3 \langle n^2 \rangle N$. Here, $\langle n^2 \rangle$ is the average value of the squared density per spin state and L_3 (L_1) is the three-body (one-body) atom-loss rate coefficient. The density distribution in the trap is well described by a thermal distribution so that

$$\frac{dN}{dt} = -L_1 N - \gamma \frac{N^3}{T^3} \qquad (1)$$

where $\gamma = L_3 (m\bar{\omega}^2 / 2\pi k_B)^3 / \sqrt{27}$ and $\bar{\omega} = (\omega_x \omega_y \omega_z)^{1/3}$. Following Ref. [37], we model the temperature increase in the gas as arising from "anti-evaporation" (the preferential loss of the highest density atoms) and recombination heating T_h which causes the temperature of the atoms to evolve as

$$\frac{dT}{dt} = \gamma \frac{N^2}{T^3} \frac{(T + T_h)}{3} \qquad (2)$$

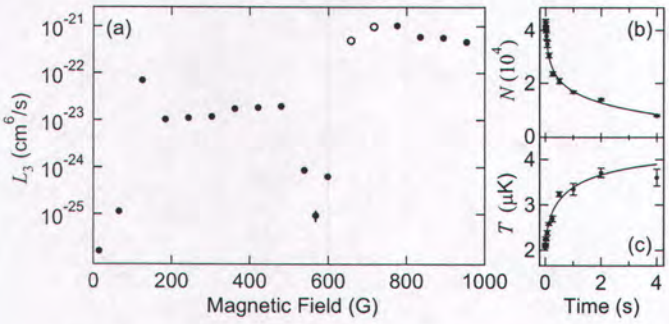

FIG. 3: (a) Three-body atom-loss rate coefficients, L_3, at various magnetic field values. Evolution of (b) atom number and (c) temperature at a particular field (180 G). The solid lines show a best-fit to the experimental data which determines L_3.

For a given set of parameters ($N(0)$, $T(0)$, L_1, L_3 and T_h), these two coupled differential equations can be numerically integrated to give $N(t)$ and $T(t)$. The best-fit parameters for a data set at a given field are determined by minimizing χ^2 with respect to these fit parameters. For example, Fig. 3 shows the measured number (b) and temperature (c) as a function of time at the field 180 G with the best-fit curves. The best-fit L_3 values at various fields are displayed in Fig. 3(a).

As shown in Fig. 3(a), L_3 varies by over four orders of magnitude and corroborates the features observed in Fig. 2(a). The error bars (typically comparable to the circles) indicate the uncertainty in the determination of L_3 due to statistical fluctuations and do not include a systematic fractional uncertainty in L_3 of $\pm 70\%$ arising from our fractional uncertainty in atom number ($\pm 30\%$) and trap frequencies ($\pm 5\%$). In the range $600\,\mathrm{G} < B < 750\,\mathrm{G}$, the L_3 values (○) may be overestimates since the measured decay includes loss events we observe in two-state mixtures at these field values. Near 0 and 568 G, three-body recombination rates are relatively small and very stable three-state Fermi gases can be created. For $L_3 = 10^{-25}\,\mathrm{cm}^6/\mathrm{s}$, a gas with a density $n = 5\times10^{11}\,\mathrm{cm}^{-3}$ per spin state has a calculated lifetime $\sim$ 40 seconds. Consistent with the data shown in Fig. 2(a), a resonant peak in L_3 is observed at $B \simeq 127\,\mathrm{G}$. The highest L_3 value we report ($10^{-21}\,\mathrm{cm}^6/\mathrm{s}$) occurs at 775 G and is likely unitarity limited (at these fields $T \simeq 6\,\mu\mathrm{K}$ due to heating and $\sqrt{\hbar^2/mk_BT} = 2200a_0$). We observe that L_3 decreases by a factor of $\simeq 2.5$ as the field is increased from 775 to 953 G, the highest field we currently access. This trend suggests that L_3 may decrease further in the high field limit where a_{12}, a_{23}, $a_{13} \to -2140a_0$.

In conclusion, we can create long-lived three-state DFGs of ^{6}Li atoms over a range of fields. Additionally, the minimal two-body loss we observe makes this system promising for future studies of Efimov trimers and other three-body bound states. Indeed, the loss resonance at 127 G may be a signature of such a state. The recombination rates at high fields need not preclude experiments designed to study color superfluidity and trion formation [18]. For instance, by working at low density ($n \sim 5\times10^{10}\,\mathrm{cm}^{-3}$) and using large period ($d \simeq 2\,\mu\mathrm{m}$) optical lattices, long lifetimes ($\gtrsim 0.1\,\mathrm{s}$) and strong interactions can simultaneously be achieved.

This material is based upon work supported by the AFOSR (Award No. FA9550-08-1-0069), the ARO (Award No. W911NF-06-1-0398) and the NSF (Award No. PHY 07-01443).

* kohara@phys.psu.edu

[1] C. A. Regal *et al.*, Phys. Rev. Lett. **92**, 040403 (2004).
[2] M. W. Zwierlein *et al.*, Phys. Rev. Lett. **92**, 120403 (2004).
[3] J. Kinast *et al.*, Phys. Rev. Lett. **92**, 150402 (2004).
[4] C. Chin *et al.*, Science **305**, 1128 (2004).
[5] T. Bourdel *et al.*, Phys. Rev. Lett. **93**, 050401 (2004).
[6] M. W. Zwierlein *et al.*, Nature **435**, 1047 (2005).
[7] G. B. Partridge *et al.*, Phys. Rev. Lett. **95**, 020404 (2005).
[8] G. B. Partridge *et al.*, Science **311**, 503 (2006).
[9] G. B. Partridge *et al.*, Phys. Rev. Lett. **97**, 190407 (2006).
[10] M. W. Zwierlein *et al.*, Science **311**, 492 (2006).
[11] Y. Shin *et al.*, Phys. Rev. Lett. **97**, 030401 (2006).
[12] M. W. Zwierlein *et al.*, Nature **442**, 54 (2006).
[13] A. G. K. Modawi and A. J. Leggett, Journal of Low Temperature Physics **109**, 625 (1997).
[14] C. Honerkamp and W. Hofstetter, Phys. Rev. B **70**, 094521 (2004).
[15] L. He *et al.*, Phys. Rev. A **74**, 033604 (2006).
[16] T. Paananen *et al.*, Phys. Rev. A **73**, 053606 (2006).
[17] P. F. Bedaque *et al.*, arXiv:cond-mat/0602525 (2006).
[18] A. Rapp *et al.*, Phys. Rev. Lett. **98**, 160405 (2007).
[19] E. Braaten and H.-W. Hammer, Ann. Phys. **322**, 120 (2007).
[20] H. Zhai, Phys. Rev. A **75**, 031603(R) (2007).
[21] R. W. Cherng *et al.*, Phys. Rev. Lett. **99**, 130406 (2007).
[22] X. W. Guan *et al.*, Phys. Rev. Lett. **100**, 200401 (2008).
[23] X.-J. Liu *et al.*, Phys. Rev. A **77**, 013622 (2008).
[24] T. Luu and A. Schwenk, Phys.Rev.Lett. **98**, 103202 (2007).
[25] S. Capponi *et al.*, Phys. Rev. A **77**, 013624 (2008).
[26] J. L. Roberts *et al.*, Phys. Rev. Lett. **85**, 728 (2000).
[27] T. Kraemer *et al.*, Nature **440**, 315 (2006).
[28] C. A. Regal, Ph.D. thesis, University of Colorado, Boulder (2005).
[29] C. H. Schunck *et al.*, Nature **454**, 739 (2008).
[30] J. Williams *et al.*, Bull. Am. Phys. Soc. **53**, 80 (2008).
[31] T. B. Ottenstein *et al.*, arXiv:0806.0587 (2008).
[32] This resonance was first reported in Ref.[31].
[33] M. Bartenstein *et al.*, Phys. Rev. Lett. **94**, 103201 (2005).
[34] K. M. O'Hara *et al.*, Science **298**, 2179 (2003).
[35] We determine trap frequencies by observing dipole oscillations (ω_y) and parametric excitation loss (ω_x, ω_z).
[36] Three particles strongly interact even if one of the pairwise scattering lengths is small since the third particle acts as a mediator for the weakly interacting pair.
[37] T. Weber *et al.*, Phys. Rev. Lett. **91**, 123201 (2003).

DEPARTMENT OF THE AIR FORCE
AIR FORCE OFFICE OF SCIENTIFIC RESEARCH (AFOSR)
875 North Randolph Street, Arlington, VA 22203-1768

Air Force Office of Scientific Research
ATTN: Matsuura - NE
875 North Randolph Street
Suite 325, Room 3112
Arlington, Virginia 22203-1768

16 JUL 2007

Dr Kenneth O'Hara
Pennsylvania State University
Physics
104 Davey Laboratory
University Park, PA 16802

Dear Dr O'Hara

It is a pleasure to inform you that your proposal "QUANTUM SIMULATION OF THE HUBBARD MODEL USING ULTRA-COLD ATOMS", is being recommended for sponsorship.

You should understand that our plans are contingent upon expected appropriations and anticipated allocations of required funds. This letter may therefore not be regarded as an authorization for the commitment of expenditure of funds. Our Directorate of Contracts will contact your business office to initiate negotiations leading to an agreement to expend funds.

Should any questions arise pertaining to the start date or other procurement matters, please address your inquiries to the Director of Contracts. Should any questions arise that concern the scientific aspects of the research, please address your inquiries to Dr Anne Matsuura, telephone 703-696-6204.

Thank you for your interest in the research program of the Air Force Office of Scientific Research.

Sincerely

Patrick G. Carrick
Director
Physics and Electronics